Analysis of Stripline-Fed Slot-Coupled Patch Antennas with Vias for Parallel-Plate Mode Suppression

Arun Bhattacharyya, *Senior Member, IEEE*, Owen Fordham, and Yaozhong Liu

***Abstract*— The paper presents an analysis of slot-coupled stripline-fed patch antennas with vias around the slot to minimize the power launched into the parallel-plate mode. A moment-method scattering formulation is invoked to include the effect of vias on the impedance characteristics of the antenna. Coupling between the stripline feed and the ground-plane slot is obtained by invoking reciprocity. Two design examples were fabricated and the measured input impedances verify the accuracy of the analysis. Vias considerably modify the impedance and resonant characteristics of a patch antenna. Radiation efficiency of patch antennas with and without vias is studied and proper location of the vias is shown to drastically reduce power in the parallel-plate mode.**

***Index Terms*—Microstrip antennas, stripline-fed, vias.**

I. Introduction

THE slot-coupled patch is an attractive radiating element for phased arrays since it is simple to fabricate and the feed circuit does not disturb the radiation patterns [1]–[8]. There is an increasing demand to integrate patch antennas with monolithic microwave integrated circuit (MMIC) devices such as phase shifters and solid-state power amplifiers (SSPA's) for phased-array applications. The MMIC's are typically placed underneath the ground plane of the patches to allow direct interface with a heat sink. The input ports of the SSPA's often must be isolated from the feed circuit with another ground plane to avoid potential feed-back/oscillation problems. However, introduction of this second ground plane allows parallel-plate modes to exist in the feed circuit layers, which have a "stripline" configuration. The lowest order parallel-plate mode has zero cutoff frequency. When a significant amount of power is launched into the parallel-plate modes, the radiation efficiency of the patch antenna is reduced. Also, the parallel-plate mode can cause mutual coupling between elements of the array, which may alter the amplitude and phase distributions from their intended values.

In a stripline-fed slot-coupled patch antenna, the parallel-plate modes are excited at the slot discontinuity in the upper ground plane. A practical way to suppress the parallel-plate modes without significantly affecting the stripline mode is to introduce conducting vias around the slot. However, the input impedance of the patch antenna changes significantly due to scattering of the parallel-plate mode from the vias. To design for first-pass success, the effect of the vias must be included in the analysis.

Many investigators have developed accurate analyses of microstrip-fed slot-coupled patch antennas [1]–[8]. Only empirical results have been reported for slot-coupled patch antennas with "stripline" feeds and mode-suppressing vias [9]. Analysis of vias used for interconnecting striplines/microstriplines is reported in [10]. In [11], experimental results for a stripline-fed slot coupled patch antenna with mode-suppressing vias are reported. However, no analysis of the mode-suppressing vias is presented. In this paper, we introduce a model to analyze stripline-fed slot-coupled patch antennas with vias around the slots. The strip is located at the interface of two dielectric layers. To obtain a reasonable coupling between the stripline and the slot, the upper dielectric layer (slot side) should be thinner and of higher permittivity than the lower dielectric layer. Such an asymmetric stripline feed sustains microstrip-like fields, but vias are still required to suppress the parallel-plate mode.

Our formulation applies the method of moments (MoM) with Galerkin's procedure in the spectral domain. The entire problem is divided into two coupling problems: 1) coupling between the slot and the stripline feed in the presence of vias and 2) coupling between the slot and the patch. The vias are modeled as cylindrical scatterers with ground planes at both ends. To make the analysis accurate, the fields on the slot aperture are represented by several mutually orthogonal modes. Lorentz's reciprocity theorem is then invoked to construct a generalized equivalent circuit for the coupling between the slot modes and the feed line. The interaction between the slot and the open end of the strip line is ignored; thus, our solution is not a full moment solution. The equivalent circuit consists of a generalized transformer and two generalized shunt admittances (admittance matrices). One admittance matrix represents radiation from the slot on the feed side of the ground plane and includes the effect of scattering from the vias. The other admittance matrix represents radiation on the patch side of the ground plane and includes the scattering from the patch metallization. A general matrix formulation is presented to handle the scattering problems in both sides, and the input impedance seen by the feed line is deduced from the equivalent circuit. To verify the accuracy of the formulation, comparisons between computed and measured impedances are presented.

Manuscript received August 13, 1996; revised December 19, 1997.

The authors are with Hughes Space and Communications, Los Angeles, CA 90009 USA.

Publisher Item Identifier S 0018-926X(98)02681-7.

II. Coupling Between Slot and Feed Line

The geometry of a slotline-fed aperture-coupled patch is shown in Fig. 1. To determine the electromagnetic coupling between the slot and the feed line, we assume that the feed line extends from $-\infty$ to $+\infty$ along x and place the slot axis along y. We then use Lorentz's reciprocity theorem [12] to construct the equivalent circuit. The electric field in the slot is expressed as

$$\vec{E}_{\text{slot}} = \sum_n V_{sn}\, \vec{e}_{sn}(x,\, y) \tag{1}$$

where V_{sn} is the modal voltage and $\vec{e}_{sn}$ is the modal voltage vector [13] for the nth waveguide mode.[1] The modal voltage vectors are orthonormal so that

$$\iint_{\text{slot}} \vec{e}_{sn}(x, y).\vec{e}_{sm}(x,\, y)\, dx\, dy = \delta_{mn} \tag{2}$$

where δ_{mn} is the Kronecker delta. The voltage discontinuity across the slot can be determined by invoking Lorentz's reciprocity theorem [12]. Following the procedure detailed in [2], [7], the discontinuity in the modal voltage ΔV is derived to be

$$\Delta V = \sum_n T_n V_{sn} \tag{3}$$

where

$$T_n = -t\, \frac{\sin(\beta_m t/2)}{\beta_m t/2} \int_{-l/2}^{l/2} \vec{e}_{sn} \times \vec{h}_m.\hat{z}\, dy \tag{4}$$

and l and t are the length and width of the slot, β_m is the propagation constant of the feed line, and $\vec{h}_m$ is the modal magnetic field vector of the feed line. In deriving T_n, the slot is assumed to be narrow and the slot's field to be uniform along x. Fig. 2 shows the circuit representation of (3). In the equivalent circuit the column matrix $[V_s]$ represents the modal amplitudes of the voltage across the slot. Note that the turns ratio of the transformer is a row matrix, according to (3). A lumped admittance matrix must be added to account for radiation from the slot into the feed layers (power coupled into undesired guided-wave modes). Another admittance (matrix) represents power coupled to the patch. In the following section, the admittance of the slot due to radiation into the feed layers will be considered.

III. Galerkin's Procedure for Slot Admittance

In this section, we invoke Galerkin's procedure to formulate the feed-side admittance of the slot in the presence of conducting vias. The top-view of a slot with vias is shown in Fig. 3. We assume uniform current distribution on the outer surface of each via. The formulation can easily be extended for several basis functions on each via. However, a uniform current distribution assumption is reasonable, because the feed layers are usually electrically thin (less than 0.1λ), which does not allow the longitudinal current to vary rapidly along the via axis. Furthermore, stationary expressions are used to obtain

[1]We consider the slot as a rectangular waveguide, carrying several waveguide modes.

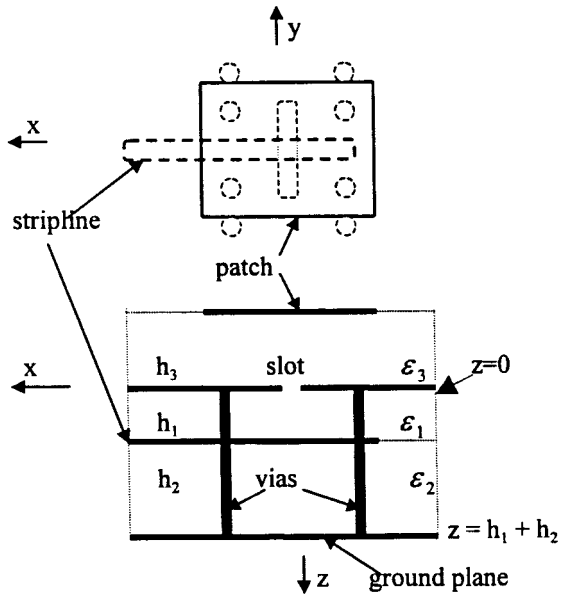

Fig. 1. Top view and side view of a stripline-fed slot-coupled patch element with vias for parallel-plate mode suppression.

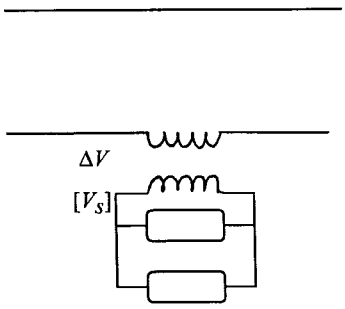

Fig. 2. Equivalent circuit representation of the patch antenna in Fig. 1.

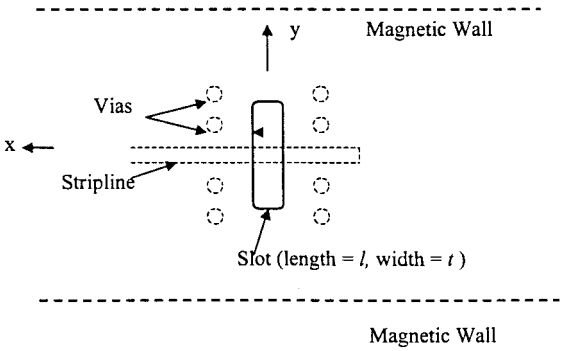

Fig. 3. Arrangement of vias around a ground plane slot.

the self and mutual impedances, therefore, the final results are insensitive to small errors in the via current distribution. Let $I_i,\ i = 1,\ 2,\ 3,\ \cdots,\ N$ be the current amplitudes induced on N vias by the slot aperture fields. Then, using Galerkin's test procedure, we obtain the following equations:

$$\sum_{j=1}^{N} I_j \langle i,\, j\rangle + \langle i,\, s\rangle = 0, \qquad i = 1,\, 2,\, \cdots,\, N \tag{5}$$

where $\langle i,\, j\rangle$ is the mutual reaction between the ith and jth vias and $\langle i,\, s\rangle$ is the mutual reaction between the slot and the ith via, with the via current amplitudes set to unity. The mutual reaction between the slot and ith via can be expressed in terms of the slot modal voltages as

$$\langle i,\, s\rangle = \sum_n V_{sn}\langle i,\, s_n\rangle \tag{6}$$

where $\langle i,\, s_n\rangle$ is the mutual reaction between the ith via and the electric field of the nth waveguide mode spanning the slot. The reaction terms will be deduced later. Substituting (6) in (5) we obtain the following matrix equation:

$$[Rv][I] = -[SI][Vs] \tag{7}$$

where $[Rv]$ is a square matrix with elements consisting of self and mutual reactions between via currents and $[SI]$ is a rectangular matrix with elements that are mutual reaction terms between slot modes and via currents. $[I]$ is the current amplitude vector for the vias and $[Vs]$ is the modal voltage vector across the slot surface. From (7) the unknown current amplitude vector can be found in terms of the slot modal voltage as

$$[I] = -[Rv]^{-1}[SI][Vs]. \tag{8}$$

The reaction between the vias and field across the slot is given by

$$\langle \text{Vias, Slot}\rangle = [I]^T[SI][Vs]. \tag{9}$$

We substitute (8) into (9) to obtain

$$\langle \text{Vias, Slot}\rangle = -[Vs]^T[SI]^T[Rv]^{-1}[SI][Vs]. \tag{10}$$

Note that $[Rv]^T = [Rv]$ because $[Rv]$ is a symmetric matrix. Therefore, the contribution of the vias to the admittance matrix of the slot is

$$[Ysv] = [SI]^T[Rv]^{-1}[SI]. \tag{11}$$

The total admittance matrix seen by the slot is

$$[Y\,\text{slot}] = [Ysv] + [Yss] \tag{12}$$

where $[Yss]$ is the self-admittance matrix of the slot whose elements are the self and mutual reactances between the orthonormal slot modes. Equation (11) holds if more than one basis function is used to represent the current on a via. In that case, the order of the $[Rv]$ matrix would be increased to $Np \times Np$, where p is the number of basis functions used for each via current. The order of $[SI]$ matrix would increase accordingly.

A. Self and Mutual Reactions of Vias

A uniform surface current on a cylindrical via can be expressed as

$$\vec{I} = \frac{I_0}{2\pi r}\,\delta(\rho - r)\hat{z} \tag{13}$$

where I_0 is the total current on a via, r is the via's outer radius, and $\rho = 0$ is the location of the via's center.

In practical feeds, the vias pass through an asymmetric two-layered dielectric structure, so a multilayered analysis is necessary. The z-directed via currents will not produce any TE_z mode [14, p. 10], therefore, we need to consider the TM_z mode fields only. The TM_z field components can be constructed from the z component of the electric displacement vector D_z [14]. In the two-layered structure bounded by ground planes at $z = 0$ and $z = h_1 + h_2$ (Fig. 1), D_z can be expressed as

$$D_z = \begin{cases} AH_0^{(2)}(k_\rho\rho)\,\cos(k_{1z}z), & z < h_1 \\ BH_0^{(2)}(k_\rho\rho)\,\cos\{k_{2z}(z - h_1 - h_2)\}, & z > h_1 \end{cases} \tag{14}$$

with $k_{1z} = \sqrt{k_0^2\varepsilon_1 - k_\rho^2}$ and $k_{2z} = \sqrt{k_0^2\varepsilon_2 - k_\rho^2}$. The above expression is valid for the region $\rho > r$. In the region $\rho < r$, the Hankel function $H_0^{(2)}(.)$ should be replaced by the Bessel function $J_0(.)$. Continuity of D_z at $z = h_1$ gives a relation between A and B. From D_z, we can find the magnetic field components in each region. Continuity of the tangential magnetic field at $z = h_1$ yields the following transcendental equation:

$$\frac{k_{1z}}{\varepsilon_1}\,\tan(k_{1z}h_1) + \frac{k_{2z}}{\varepsilon_2}\,\tan(k_{2z}h_2) = 0. \tag{15}$$

The above equation can be solved numerically for k_ρ. Each real root corresponds to a propagating parallel-plate mode. Considering all possible TM_z parallel-plate modes, the displacement vector component D_z can be written as

$$D_z = \begin{cases} \displaystyle\sum_i A_i H_0^{(2)}(k_{\rho i}\rho) f_i(z), & \rho > r \\ \displaystyle\sum_i B_i J_0(k_{\rho i}\rho) f_i(z), & \rho < r \end{cases} \tag{16}$$

where

$$f_i(z) = \begin{cases} \cos(k_{1zi}z), & z < h_1 \\ \dfrac{\cos(k_{1zi}h_1)}{\cos(k_{2zi}h_2)}\,\cos\{k_{2zi}(z - h_1 - h_2)\}, & z > h_1 \end{cases} \tag{17}$$

and $k_{\rho i}$ is the ith solution of (15). It can be shown that $f_i(z)$ forms a complete set of orthogonal functions [14, p. 68], with the orthogonal relation given by

$$\int_0^h \frac{f_i(z)f_j(z)}{\varepsilon(z)}\,dz = 0, \qquad i \neq j,\, h = h_1 + h_2. \tag{18}$$

This orthogonal relation is used to expand the via current in terms of the parallel-plate mode functions. After algebraic manipulation, the expression for A_i in (16) is obtained as

$$A_i = I_0\left[\frac{k_{\rho i}^2 T_{1i}}{4\omega T_{2i}}\,J_0(k_{\rho i}r)\right] = I_0 K_i \tag{19}$$

where K_i represents the quantity inside the square bracket. T_{1i} and T_{2i} are integrals given by

$$T_{1i} = \int_0^h f_i(z)/\varepsilon(z)\,dz \tag{20}$$

$$T_{2i} = \int_0^h f_i^2(z)/\varepsilon(z)\,dz. \tag{21}$$

For a two-layered medium bounded by ground planes at $z = 0$ and $z = h_1+h_2$, T_{1i}, and T_{2i} have the following closed forms:

$$T_{1i} = \cos(k_{1z\,i}h_1)[\tan(k_{1zi}h_1)/(k_{1zi}\varepsilon_1) + \tan(k_{2zi}h_2)/(k_{2zi}\varepsilon_2)] \quad (22)$$

$$T_{2i} = \frac{h_1}{2\varepsilon_1}[1 + Sn(2k_{1zi}h_1)] + \frac{h_2}{2\varepsilon_2}[1 + Sn(2k_{2zi}h_2)]\frac{\cos^2(k_{1zi}h_1)}{\cos^2(k_{2zi}h_2)} \quad (23)$$

where $Sn(x) = \sin(x)/x$. The self reaction of a via is given by

$$\langle I_0,\, I_0\rangle = -I_0^2 \sum_i K_i H_0^{(2)}(k_{\rho i} r) T_{1i}. \quad (24)$$

The mutual reaction between two vias of currents I_1 and I_2 is derived as

$$\langle I_1,\, I_2\rangle = -I_1 I_2 \sum_i K_i \frac{1}{2\pi r} \oint_{\text{via2}} T_{1i} H_0^{(2)}(k_{\rho i}\rho_{12})\, dl \quad (25)$$

where ρ_{12} is the distance between the center of via 1 to a surface point of via 2. The integration is taken around the contour of via 2. If the vias are sufficiently separated from each other such that $r \ll \rho_{12}$, the mutual reaction simplifies to

$$\langle I_1,\, I_2\rangle = -I_1 I_2 \sum_i K_i H_0^{(2)}(k_{\rho i} r_{12}) T_{1i} \quad (26)$$

where r_{12} is the center-to-center distance between the two vias and K_i is defined in (19). The normalized mutual reaction for use in (5) is given by

$$\langle i,\, j\rangle = \frac{\langle I_i,\, I_j\rangle}{I_i\, I_j} = -\sum_i K_i H_0^{(2)}(k_{\rho i} r_{12}) T_{1i}. \quad (27)$$

B. Mutual Reaction Between a Via and the Slot

The mutual reaction between current on a via and a modal field on the slot is defined as

$$\langle \text{Via},\, s_n\rangle = \iint_{\text{slot}} (\vec{e}_{sn} \times \vec{H}_v).\hat{z}\, dx\, dy \quad (28)$$

where $\vec{e}_{sn}$ is the modal electric field vector for the nth slot mode and $\vec{H}_v$ is the magnetic field vector produced by the via current. The magnetic field vector can be determined from D_z in (16) using the procedure detailed in [14]. For the slot shown in Fig. 3, the aperture field is directed along x; therefore, the y component of the via's magnetic field is of interest. At the slot location, this component of the via's magnetic field is

$$H_{vy} = j\omega \sum_i A_i H_1^{(2)}(k_{\rho i}\, r)\, \frac{x}{k_{\rho i}\rho}. \quad (29)$$

The via is assumed to be located at $p = 0$. Equation (29) is substituted into (28) for H_{vy} and the final expression for the mutual reaction becomes

$$\langle Via,\, s_n\rangle = j\omega x_s t \sum_i \frac{A_i}{k_{\rho i}} \int_{y_s - l/2}^{y_s + l/2} \cdot e_{snx} \frac{H_1^{(2)}\left(k_{\rho i}\sqrt{x_s^2 + y^2}\right)}{\sqrt{x_s^2 + y^2}}\, dy. \quad (30)$$

In (30), $(x_s,\, y_s)$ is the relative coordinate of the slot's center with respect to the via-center. The slot is assumed to be electrically narrow. The above equation is used for $\langle i,\, s_n\rangle$ in (6), with A_i given by (19) and I_0 set to unity.

C. Self Reaction of the Slot

To find the $[Yss]$ term in (12), we need to obtain the self-reactions between the modal fields on the slot. We introduce two infinitely long magnetic walls on either side of the slot, running perpendicular to the slot axis as shown in Fig. 3. In the presence of these fictitious magnetic walls, the parallel-plate modes become plane waves as opposed to cylindrical waves, which simplifies the analysis considerably. If the magnetic walls are several wavelengths away from the slot location, the self-reaction computation will be sufficiently accurate for most applications.

The electric field of the nth mode in a narrow slot can be expressed as

$$\vec{e}_{sn} = \hat{x} e_{snx}. \quad (31)$$

The equivalent magnetic current is given by

$$M_n = \hat{x} \times \hat{z} e_{snx}\delta(z) = \hat{y} M_{yn}\delta(z) \quad -t/2 < x < t/2. \quad (32)$$

The magnetic current component can be expanded in a Fourier series as

$$M_n = \hat{y} \sum_i M_{yn}^{(i)} \cos(2\pi i y/w)\delta(z) \quad (33)$$

where w is the separation between two fictitious magnetic walls. Now consider a magnetic line current at $x = x_0$, represented by

$$m_{yi} = \hat{y}\delta(x - x_0) \cos(2\pi i y/w)\delta(z). \quad (34)$$

Using a mode-matching procedure, the magnetic field produced by the above magnetic line current is given by

$$h_{yi}(x,\, y,\, z;\, x_0) = \frac{\omega\, k_{xi}}{2k_{\rho 1}^2 T_{21}} \exp\{\mp jk_{xi}(x - x_0)\} \cdot \cos(2\pi i y/w). \quad (35)$$

The $+$ and $-$ signs correspond to $x > x_0$ and $x < x_0$ regions, respectively. T_{21} is the integral defined in Section III-A. $k_{\rho 1}$ is the lowest order zero of (15) and $k_{xi} = \sqrt{k_{\rho 1}^2 - (2\pi i/w)^2}$. To obtain this result, we assumed that only the lowest order TM_z mode is excited, which is valid for thin dielectric layers. Using superposition, the magnetic field produced by the nth slot mode is

$$H_{yn} = \sum_i M_{yn}^{(i)} \cos(2\pi i y/w) \int_{-t/2}^{t/2} h_{yi}(x,\, y,\, z;\, x_0)\, dx_0. \quad (36)$$

The mutual admittance between the mth and nth slot modes is given by

$$Yss(m,\, n) = \iint_{\text{slot}} e_{xm}\, H_{yn}\, dx\, dy. \quad (37)$$

After double integration we obtain

$$Yss(m,\ n) = \sum_i \frac{-2\omega\varepsilon_0 E_m^{(i)} E_n^{(i)}}{k_{xi} k_{\rho 1}^2 w \sigma_i T_{21}} \cdot [1 - jk_{xi}t - \exp(-jk_{xi}t)] \tag{38}$$

where $\sigma_0 = 2$, $\sigma_i = 1$, $i \neq 0$. $E_m^{(i)}$ is given by

$$E_m^{(i)} = \frac{2}{w\sigma_i} \int_{-l/2}^{l/2} e_{xm}\ \cos(2\pi iy/w)\, dy. \tag{39}$$

The above expression for $Yss(m,\ n)$ defines the elements of $[Yss]$ in (12).

IV. Input Impedance

To find the input impedance seen by the feed line, we determine the patch-side admittance of the slot. We use the same procedure as in Section III. In this case, the equivalent slot-admittance matrix can be expressed as

$$[Y\text{slot}'] = [Ysp] + [Yss'] \tag{40}$$

where the prime denotes the admittance for the patch side. $[Yss']$ is the patch side self-admittance matrix of the slot modes if the patch metallization is not present. Following (11), $[Ysp]$ is given by

$$[Ysp] = [SP]^T [Rp]^{-1} [SP] \tag{41}$$

where $[SP]$ is the mutual reaction matrix between slot modes and the current basis functions on the patch surface and $[Rp]$ is the self- and mutual-reaction matrix between various current basis functions on the patch surface. To obtain the elements of these matrices, we apply the spectral-domain technique. The fields are expressed in terms of infinite Sommerfeld-type integrals for an isolated patch [1], [2], [7], [8], while Floquet modal fields are used for an infinite patch array [15].

The input impedance seen by the feed line can be obtained directly from the equivalent circuit shown in Fig. 2. The input impedance is given by

$$\frac{1}{Z_{\text{in}}} = [T]^T \{[Y\text{slot}] + [Y\text{slot}']\}[T] \tag{42}$$

where the elements of the column matrix $[T]$ can be obtained from (4). The $[Y\text{slot}]$ and $[Y\text{slot}']$ matrices are given in (12) and (40), respectively.

V. Results and Discussions

The entire formulation was programmed in FORTRAN and used to design stripline-fed slot-coupled patch arrays for a 20-GHz application. A rexolite substrate was chosen for the patch layer. The feed strip was located at the interface of two different substrates: TMM-10 between the strip and the slot's ground plane and TMM-3 between the strip and the bottom ground plane. The asymmetric stripline structure was necessary to yield reasonable input resistance for the patch antenna.

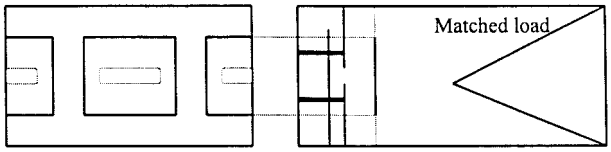

Fig. 4. Waveguide simulator for active impedance measurement.

We measured the active input impedances of two patch arrays using the waveguide simulator technique [15]. A rectangular waveguide was fabricated with a and b dimensions corresponding to two and one element spacings, respectively. One end of the waveguide contained a slot-coupled patch centered in the cross-section, with the waveguide wall shorted by the patch ground plane. Two passive half-patches on either side were shorted to the narrow walls of the waveguide. The arrangement is shown in Fig. 4 and is equivalent to the environment in an infinite array scanned to 24° in the H-plane. The waveguide was terminated in a good match using a tapered absorber. A stripline-to-coaxial transition was connected to the feed to interface with the vector network analyzer. LRL calibration was used to de-embed this transition and establish an accurate reference plane located at the edge of the slot.

The active input impedance of the patches was computed at the 24° scan angle. The eight vias nearest to the slot were included in the analysis of the stripline-slot coupling. On the patch side, the reaction computations in (41) used Floquet modal analysis with 600 Floquet modes. Three slot modes were included for the numerical results presented here. However, subsequent numerical tests showed that a single slot mode provided similar accuracy. Fig. 5(a) and (b) shows the comparison between computed and measured results for two different patch/slot dimensions in a waveguide simulator. The reference plane for impedance measurements (and computations) was considered to be the source edge of the slots (instead of the slot center). In both cases the agreement between the computed and measured data found to be good.

To find the effect of vias on input impedance, we computed the impedance of a patch for three different feed configurations: 1) the feed in array environment and no vias; 2) fed in isolation with no vias; and 3) fed with eight vias around the slot. Fig. 6 shows the impedances for the three-feed configurations. The impedance levels and resonant frequencies differ considerably from each other. The profound effect of vias on input impedance is apparent in the comparison.

Motivated by these results, we used the numerical model to study the effect of vias on the impedance characteristics of a patch array. We computed the active input impedance with four vias (dia. $= 0.096$ cm) placed symmetrically with respect to the slot axes. Three different curves in Fig. 7 resulted from three different locations of the vias. The resonant frequency (defined as the frequency corresponding to the peak input resistance) and resistance depend strongly on the distance from the vias to the slot. As the vias approach the center of the slot, the resonant frequency increases considerably. This phenomenon can be explained physically. Resonance occurs

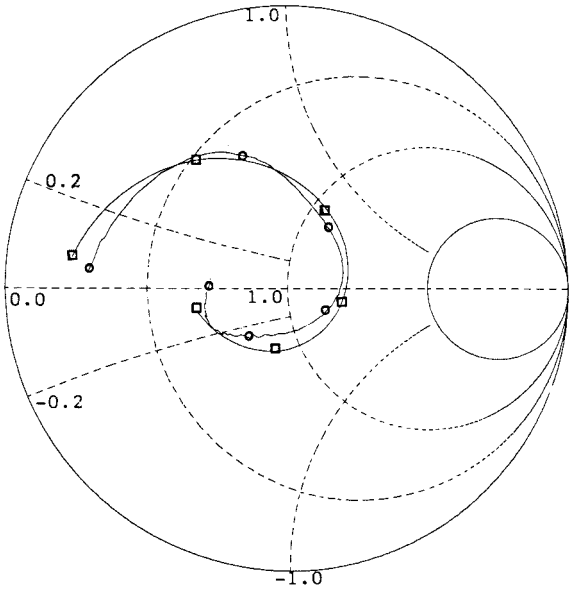

(a)

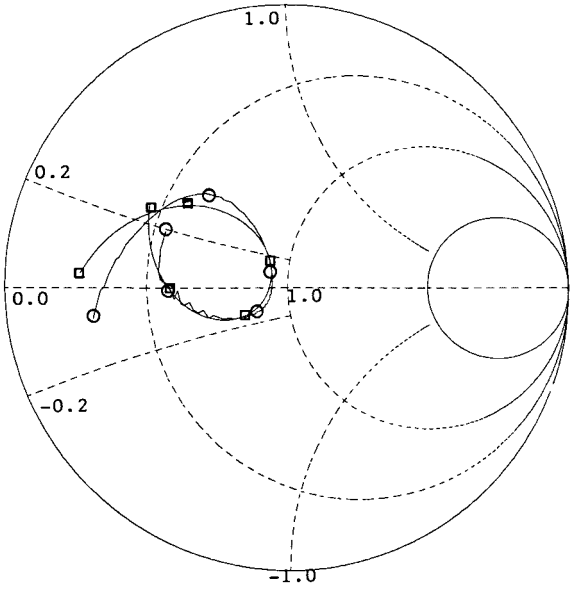

(b)

Fig. 5. Computed and measured active impedance of a patch in a waveguide simulator shown in Fig. 4. Element spacing = 0.876 cm × 0.876 cm, $h_1 = 0.038$ cm, $h_2 = 0.0635$ cm, $\varepsilon_1 = 9.8$, $\varepsilon_2 = 3.27$, $\varepsilon_3 = 2.53$, 50-Ω strip line. With respect to the slot center, the via coordinates for eight vias are (±0.1, ±0.3) and (±0.1, ±0.13), respectively. Via diameter = 0.096 cm, stub length = 0.0648 cm (with end effect of 0.0038 cm). Impedance computed/measured with respect to the source end of the slots. (a) Patch size 0.35 cm × 0.68 cm, patch substrate thickness = 0.084 cm, slot size 0.29 cm × 0.025 cm. (b) Patch size 0.37 cm × 0.68 cm, slot size 0.271 cm × 0.025 cm, patch substrate thickness = 0.088 cm. $f = 18$–23 GHz clockwise. —□— computed, — ∘ — measured.

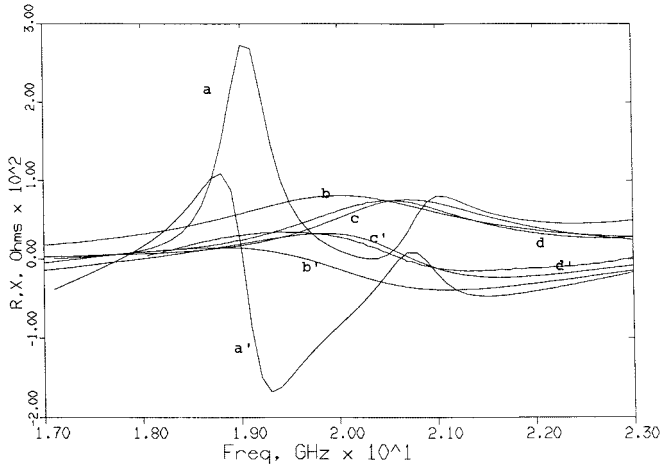

Fig. 6. Active impedance versus frequency of a patch array with different feed situations. Curve a: input resistance with no via, feed in array environment. Curve b: no via, feed in isolation. Curve c: eight vias around the slot. Curve d: measurement with eight vias. The curves denoted by primes are the corresponding input reactance counterparts. All dimensions are same as in Fig. 5(a). Scan angle = 24°.

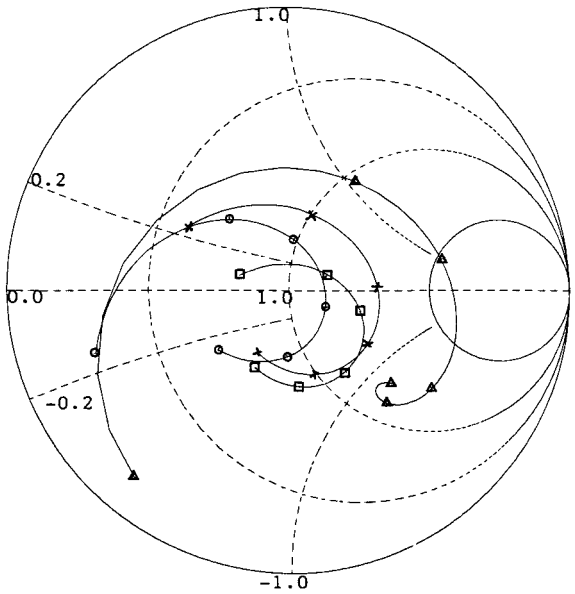

Fig. 7. Computed active input impedance of a patch antenna (in array environment) with and without vias. —△— no via and feed in array, —□— no via and isolated feed, — × — with four vias, coordinate of the vias are (±0.1, ±0.2), — ∘ — four vias, coordinate of vias are (±0.1, ±0.13). Via diameter = 0.096 cm. Patch size = 0.37 cm × 0.68 cm, slot size = 0.32 cm × 0.02 cm, array element spacing = 0.876 cm × 0.876 cm. Scan angle = 0°, remaining parameters are same as in Fig. 5. $f = 17$–22 GHz clockwise.

when the inductive reactance of the slot in the patch side is nulled by the capacitive reactance of the slot in the feed side. The vias in the feed side reduce the capacitive reactance of the slot because vias are inductive in nature. Near resonance, the patch-side reactance has a negative slope (frequency response of a typical lossy cavity). To counterbalance a smaller value of the capacitive reactance, a positive frequency shift must occur.

The effectiveness of the vias can be quantified in terms of radiation efficiency defined as: efficiency = (power coupled to patch side)/(total input power). From the equivalent circuit in Fig. 2 and (42), the efficiency can be obtained directly from the equivalent conductances on the two sides of the slot as

$$\text{Efficiency} = \frac{[T]^T[G\text{slot}'][T]}{[T]^T\{[G\text{slot}] + [G\text{slot}']\}[T]}$$

where $[G\text{slot}]$ and $[G\text{slot}']$ are the real parts of $[Y\text{slot}]$ and $[Y\text{slot}']$ matrices in (42). Note that $[G\text{slot}]$ is the summation of two matrices, as given in (12). Without vias, $[Ysv]$ should

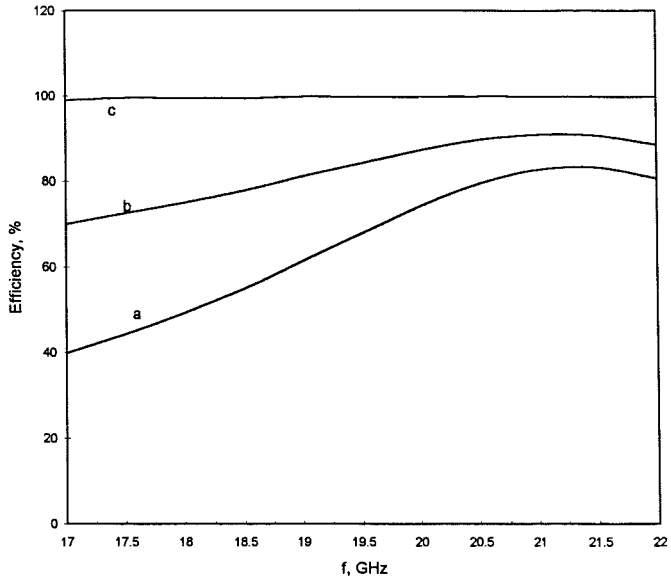

Fig. 8. Radiation efficiency versus frequency of a patch antenna with and without vias. Via coordinates are same as in Fig. 7. Curve a: no via, isolated feed, curve b: four vias at (± 0.1, ± 0.2), curve c: four vias at (± 0.1, ± 0.13). Remaining parameters are same as in Fig. 7.

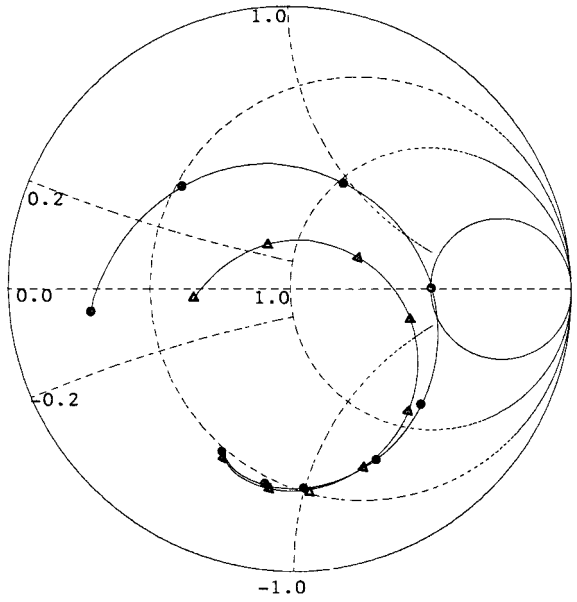

Fig. 9. Input resistance versus frequency of an isolated patch with and without vias. —o— with no vias, —△— with four vias. Via coordinates are (± 0.1, ± 0.2). Other dimensions are same as in Fig. 7. $f = 15$–23 GHz clockwise.

be set to a null matrix. The radiation efficiency was computed and plotted in Fig. 8. Without vias, the radiation efficiency near resonance ($f = 18$ GHz) is about 50%. When the vias are 0.4 cm apart, the efficiency increases to about 75%. However, when the vias are 0.25 cm apart, the radiation efficiency increases to almost 100%. In other words, the vias corresponding to curve "c" eliminate parallel-plate mode propagation.

We obtained similar effects of vias on the impedance of an isolated patch. For an isolated patch, the reactions in (41) were computed from Sommerfeld-type integrals. Fig. 9 shows the input impedance of an isolated patch with and without vias around the slot feed. Four vias were placed symmetrically with respect to the slot axes. The vias alter the input impedance of the antenna and shift the resonant frequency higher. The resistances at resonance with and without vias are 154 and 118 Ω, respectively. The corresponding resonant frequencies are 18.1 and 17.9 GHz, respectively.

VI. Conclusions

We presented a technique to analyze slot-coupled patch antennas fed by stripline with vias around the coupling slot. The accuracy of this model was verified by design, fabrication, and measurement of two antennas for a 20-GHz application. We found that vias have a profound impact on the input impedance. The mode-suppressing vias improve the radiation properties of a patch antenna in the following three ways: 1) gain improves because the available power for radiation increases; 2) for array applications, parasitic mutual coupling caused by the parallel-plate mode is eliminated; and 3) edge diffraction due to the parallel-plate mode is eliminated.

The model presented here is useful for active array applications where a stripline feed is required to isolate the feed circuitry from the active devices. At higher frequencies, smaller via-spacing must be used around the slot to insure that parallel-plate mode resonances do not occur. The effect of the vias on the input impedance of the antenna becomes substantial and must be included in the design tool. Our model predicts the resulting impedance values accurately enough for first-pass design success.

References

[1] P. L. Sullivan and D. H. Schaubert, "Analysis of an aperture-coupled microstrip antenna," *IEEE Trans. Antennas Propagat.,* vol. AP-34, pp. 977–984, Aug. 1986.

[2] D. M. Pozar, "A reciprocity method of analysis for printed-slot and slot-coupled microstrip antenna," *IEEE Trans. Antennas Propagat.,* vol. AP-34, pp. 1439–1445, Dec. 1986.

[3] X. Gao and K. Chang, "Network modeling of an aperture coupling between microstrip line and patch antenna for active array applications," *IEEE Trans. Microwave Theory Tech.,* vol. 36, pp. 505–512, Mar. 1988.

[4] M. I. Aksun, S. L. Chuang, and Y. T. Lo, "On slot-coupled microstrip antennas and their applications to CP operations—Theory and experiment," *IEEE Trans. Antennas Propagat.,* vol. 38, pp. 1224–1230, Aug. 1990.

[5] A. Ittipiboon, R. Oostlander, Y. M. M. Antar, and M. Cuhaci, "A modal-expansion method of analysis an measurement on aperture-coupled microstrip antenna," *IEEE Trans. Antennas Propagat.,* vol. 39, pp. 1567–1573, Nov. 1991.

[6] H. Shoki, K. Kawabata, and H. Iwasaki, "A circularly polarized slot-coupled microstrip antenna using a parasitically excited slot," in *IEEE APS Symp. Dig.,* London, Canada, June 1991, pp. 1114–1117.

[7] A. K. Bhattacharyya, Y. M. M. Antar, and A. Ittipiboon, "Spectral domain analysis of aperture-coupled microstrip antenna," *Proc. Inst. Elect. Eng.* vol. 139, pt. H, pp. 459–464, Oct. 1992.

[8] X. H. Yang and L. Shafai, "Characteristics of aperture coupled microstrip antennas with various radiating patches and coupling apertures," *IEEE Trans. Antennas Propagat.,* vol. 43, pp. 72–78, Jan. 1995.

[9] R. C. Hall and J. R. Sanford, "Performance enhancements for aperture-coupled microstrip antennas," in *IEEE APS Symp. Dig.,* Chicago, IL, July 1992, pp. 1040–1043.

[10] M. Tsai, C. Chen, T. Horng, and N. G. Alexopoulos, "Multiple arbitrary shape via-holes and air-bridge transitions in multilayered structures," in *IEEE MTT-S Dig.,* San Francisco, CA, June 1996, vol. 2, pp. 707–710.

[11] P. Brachat and J. M. Baracco, "Dual-polarization slot-coupled printed antennas fed by stripline," *IEEE Trans. Antennas Propagat.,* vol. 43, pp. 736–742, July 1995.

[12] R. E. Collin and F. J. Zucker, *Antenna Theory.* New York: McGraw-Hill, 1969, pt. 1, ch. 14.
[13] R. F. Harrington, *Time-Harmonic Electromagnetic Fields.* New York: McGraw-Hill, 1961, ch. 8.
[14] A. K. Bhattacharyya, *Electromagnetic Fields in Multilayered Structures, Theory and Applications.* Norwood, MA: Artech House, 1994.
[15] D. M. Pozar, "Analysis of an infinite phased array of aperture coupled microstrip patches," *IEEE Trans. Antennas Propagat.*, vol. 37, pp. 418–425, Apr. 1989.

Arun Bhattacharyya (M'87–SM'91), for photograph and biography, see p. 531 of the April 1996 issue of this TRANSACTIONS.

Owen Fordham was born in Chicago, IL, on November 7, 1959. He received B.S. degrees in mechanical engineering and electrical engineering from Massachusetts Institute of Technology, Cambridge, MA, in 1982, and the M.S. degree in electrical engineering from University of California, Los Angeles, in 1987. He is currently working toward the Ph.D. degree at University of California, Los Angeles.

In 1982, he joined Hughes Aircraft Company, Los Angeles, CA. His fields of interest include passive and active microwave devices and circuits.

Yaozhong Liu received the B.S. and M.S. degrees in electrical engineering from Tsinghua University, Beijing, China in 1983 and 1986, respectively, and the Ph.D. degree in electrical engineering from University of California, Los Angeles, in 1995.

He is currently a Staff Engineer at Hughes Space and Communications Company, Los Angeles, CA, where he develops microwave and millimeter-wave circuits and systems for satellite communications. His current research interests include microwave and millimeter-wave amplifiers, mixers, multilayer structures, and digital microwave communications.